International Astronomy and Astrophysics Research Journal

Volume 8, Issue 1, Page 66-79, 2026; Article no.IAARJ.163308

Spectral-Type Dependence of Habitable Zone Classification Differences in Confirmed Exoplanets: A Systematic Comparison of Temperature-Dependent and Constant-Flux Models

Aswin Karkadakattil [a*]

[a] *Independent Researcher, Kasaragod, Kerala, PIN: 671314, India.*

Author's contribution

The sole author designed, analysed, interpreted and prepared the manuscript.

Article Information

DOI: https://doi.org/10.9734/iaarj/2026/v8i1125

Open Peer Review History:
This journal follows the Advanced Open Peer Review policy. Identity of the Reviewers, Editor(s) and additional Reviewers, peer review comments, different versions of the manuscript, comments of the editors, etc are available here: https://pr.sdiarticle5.com/review-history/163308

Original Research Article

Received: 03/05/2026
Accepted: 25/07/2026
Published: 01/08/2026

Abstract

Habitable zone (HZ) boundaries are commonly estimated using either the temperature-dependent formulation of Kopparapu et al. (2013, 2014) or simplified constant-flux models that neglect stellar effective temperature. Although both approaches are widely used in exoplanet studies, their influence on habitable-zone classification across the confirmed exoplanet population has not been systematically quantified. In this study, we compare these two HZ formulations using a dataset of 1,347 confirmed exoplanets with available stellar effective temperature, stellar luminosity, and orbital semi-major axis obtained from the NASA Exoplanet Archive. The conservative Kopparapu model classifies 71 planets (5.27%) as residing within the HZ, whereas the constant-flux model identifies 46 planets (3.41%). The two approaches disagree for 39 planets, corresponding to an overall disagreement rate of 2.90% (95% CI: 2.13–3.93%). This disagreement exhibits a strong spectral-type dependence, increasing from negligible levels for A- and F-type stars to 8.33% for M-

**Corresponding author: E-mail: ashwinharik20000@gmail.com;*

Cite as: *Karkadakattil, A. (2026). Spectral-Type Dependence of Habitable Zone Classification Differences in Confirmed Exoplanets: A Systematic Comparison of Temperature-Dependent and Constant-Flux Models. International Astronomy and Astrophysics Research Journal, 8(1), 66–79. https://doi.org/10.9734/iaarj/2026/v8i1125*

dwarf systems (95% CI: 5.40–12.65%), with a statistically significant association confirmed by a chi-square test ($\chi^2 = 31.62$, $p < 0.0001$). Model-level analysis demonstrates that the observed trend originates from the temperature-dependent stellar flux correction incorporated in the Kopparapu formulation, which accounts for differences in stellar spectral energy distributions and produces the greatest divergence from the constant-flux approximation for cool stars. These findings demonstrate that simplified constant-flux HZ criteria can systematically underestimate habitable-zone candidates around M dwarfs, potentially influencing habitable-zone catalogues, target prioritisation for atmospheric characterisation, and future exoplanet habitability surveys.

Keywords: *Habitable zone; confirmed exoplanets; stellar spectral type; temperature-dependent flux; constant-flux model; M dwarfs; stellar effective temperature; planetary habitability; model comparison; target prioritization.*

1. Introduction

The habitable zone (HZ), defined as the range of orbital distances within which a rocky planet can maintain liquid water on its surface under suitable atmospheric conditions, remains one of the most widely adopted frameworks for identifying potentially habitable exoplanets (Kasting et al., 1993; Kopparapu et al., 2013). With the increasing capability of observational facilities such as the James Webb Space Telescope (JWST) and forthcoming extremely large telescopes to characterise terrestrial exoplanet atmospheres, accurate identification of HZ candidates has become increasingly important. Because atmospheric characterisation is observationally expensive, HZ classification is widely used as an initial screening criterion for prioritising targets for detailed follow-up observations (Dressing & Charbonneau, 2015; Hill et al., 2023; Lagage et al., 2026; TRAPPIST-1 JWST Community Initiative, 2024). The concept of the habitable zone has evolved substantially since its early development. Early formulations described the HZ using fixed stellar-flux limits that depended only on stellar luminosity and implicitly assumed identical radiative conditions for stars of different spectral types (Hart, 1979; Huang, 1959; Kasting et al., 1993). Subsequently, Kopparapu et al. (2013, 2014) introduced a temperature-dependent formulation in which the effective stellar flux defining each HZ boundary varies with stellar effective temperature. This refinement accounts for differences in stellar spectral energy distributions, which influence planetary atmospheric absorption, radiative balance, and greenhouse processes, and has consequently become the standard approach adopted in most contemporary HZ studies (Kopparapu et al., 2013, 2014). Recent reviews of rocky exoplanet atmospheres have further emphasised that stellar spectral energy distributions and atmosphere–radiation interactions play a central role in determining planetary climate and habitability, reinforcing the importance of temperature-dependent HZ models (Wordsworth & Kreidberg, 2022). In parallel with these theoretical developments, recent observational efforts have substantially expanded the inventory of confirmed exoplanets and habitable-zone catalogues. Studies have focused on compiling comprehensive HZ catalogues (Bohl et al., 2026; Hill et al., 2023), evaluating stellar habitable zones using observational datasets (Jiang et al., 2024), refining concepts of planetary habitability (Hall et al., 2023), and establishing strategies for atmospheric characterisation of terrestrial exoplanets using current and future space missions (Lagage et al., 2026; TRAPPIST-1 JWST Community Initiative, 2024). These advances highlight the increasing importance of reliable and consistent HZ classification for guiding observational target selection.

Recent studies indicate that habitable-zone placement is best interpreted as an initial screening criterion because the ultraviolet environment, atmospheric retention, planetary structure, and atmospheric evolution can further constrain long-term habitability (Deb et al., 2025; Spinelli et al., 2024; Van Looveren et al., 2025). The evolution and retention of terrestrial-planet atmospheres and surface-water reservoirs likewise depend on planetary properties in addition to radiative boundary estimates (Liu, 2018).

Despite the widespread use of both temperature-dependent and simplified constant-flux formulations, their practical influence on habitable-zone classification across the current population of confirmed exoplanets has not been systematically quantified. Most previous investigations have focused on developing habitable-zone models, compiling HZ planet catalogues, or examining planetary habitability around specific stellar populations (Bohl et al., 2026; Hill et al., 2023; Jiang et al., 2024; Kane et al., 2016). Comparatively little attention has been given to evaluating how the choice of HZ formulation affects classification outcomes across different stellar spectral types or to quantifying the frequency of disagreement between these commonly used approaches.

1.1 Objective of the Study

This short communication addresses this gap by comparing HZ classifications obtained from the conservative Kopparapu temperature-dependent model and a simplified constant-flux model using the current catalogue of confirmed exoplanets from the NASA Exoplanet Archive. In addition to quantifying the overall agreement between the two approaches, the study evaluates disagreement rates across stellar spectral types and investigates how these differences arise from the temperature-dependent correction incorporated in the Kopparapu formulation. Rather than proposing a new habitable-zone model, this work provides a systematic assessment of how HZ model selection influences classification outcomes across the confirmed exoplanet population, offering practical guidance for habitable-zone catalogue construction, observational target prioritisation, and future exoplanet habitability studies.

2. Data and Methods

2.1 Data Source

Stellar and planetary parameters were obtained from the NASA Exoplanet Archive Planetary Systems (ps) table through a synchronous TAP query (Akeson *et al.*, 2013). The archive was accessed on 18 July 2026. As the archive is continuously updated with newly confirmed planets and revised system parameters, this access date is reported to ensure reproducibility. The query retrieved five parameters: planet name (*pl_name*), host star name (*hostname*), stellar effective temperature (*st_teff*), stellar luminosity (*st_lum*), and planetary orbital semi-major axis (*pl_orbsmax*). Only the default parameter set for each planet (*default_flag* = 1) was retained to avoid duplicate entries arising from multiple published solutions. The initial query returned 1,353 confirmed planets. Entries missing stellar effective temperature, stellar luminosity, or orbital semi-major axis were removed. Additional quality-control filters excluded non-physical values by restricting stellar effective temperature to 2500–10000 K and requiring both stellar luminosity and orbital semi-major axis to be positive. The final dataset comprised 1,347 planets. These filters were applied only to remove incomplete or physically unrealistic records and did not impose any additional scientific selection.

2.2 HZ Model A — Kopparapu et al. (2013, 2014)

The first HZ model follows the temperature-dependent formulation proposed by Kopparapu et al. (2013), using the updated coefficients reported by Kopparapu et al. (2014). The effective stellar flux at each habitable-zone boundary was calculated as

$$S_{\mathrm{eff}} = S_{\mathrm{eff},\odot} + aT + bT^2 + cT^3 + dT^4,$$

Where

$$T = T_{\mathrm{eff}} - 5780\ \mathrm{K},$$

and $S_{\mathrm{eff},\odot}$, a, b, c, and $d$are boundary-specific coefficients.

The conservative habitable zone was adopted using the Runaway Greenhouse inner boundary with

$$S_{\mathrm{eff},\odot} = 1.107,\ a = 1.332 \times 10^{-4},\ b = 1.580 \times 10^{-8},\ c = -8.308 \times 10^{-12},\ d = -1.931 \times 10^{-15}$$

and the Maximum Greenhouse outer boundary with

$$S_{\mathrm{eff},\odot} = 0.356,\ a = 6.171 \times 10^{-5},\ b = 1.698 \times 10^{-9},\ c = -3.198 \times 10^{-12},\ d = -5.575 \times 10^{-16}$$

The corresponding habitable-zone boundary distance was calculated as

$$d = \sqrt{\frac{L}{S_{\mathrm{eff}}}},$$

where $L$is the stellar luminosity expressed in units of solar luminosity ($L_{\odot}$). A planet was classified as residing within the habitable zone when its orbital semi-major axis lay between the calculated inner and outer boundary distances.

2.3 HZ Model B — Simplified Constant-Flux Model

The second model represents a simplified constant-flux approach in which habitable-zone flux limits are assumed to be independent of stellar effective temperature. Unlike the temperature-dependent formulation described in Section 2.2, this approach adopts the solar reference effective stellar flux values reported by Kopparapu et al. (2013, 2014) and applies them uniformly to all host stars. Consequently, the stellar effective-temperature correction is omitted while the same conservative habitable-zone reference boundaries are retained, allowing the influence of stellar effective temperature on habitable-zone classification to be isolated.

The habitable-zone boundary distances were calculated as

$$d_{\text{inner}} = \sqrt{\frac{L}{1.107}},\ d_{\text{outer}} = \sqrt{\frac{L}{0.356}},$$

where $L$is the stellar luminosity expressed in units of solar luminosity ($L_{\odot}$).

This simplified formulation was included as a reference model to facilitate direct comparison with the temperature-dependent Kopparapu formulation. By retaining the same conservative solar reference effective stellar flux values while removing the stellar effective-temperature correction, the comparison isolates the effect of stellar effective temperature on habitable-zone classification.

2.4 Classification and Statistical Analysis

All 1,347 confirmed exoplanets were classified independently under both habitable-zone models using the reported stellar effective temperature, stellar luminosity, and planetary orbital semi-major axis. A disagreement case was defined as a planet that received different habitable-zone classifications under the two models. To examine the dependence of classification agreement on stellar type, planets were grouped into five spectral classes based on standard MK effective-temperature boundaries: M (<3700 K), K (3700–5200 K), G (5200–6000 K), F (6000–7500 K), and A (≥7500 K). For each spectral class, the disagreement rate was calculated as the proportion of planets receiving inconsistent classifications between the two models. Ninety-five per cent confidence intervals were estimated using the Wilson score interval, which provides stable interval estimates for binomial proportions, particularly when sample sizes are small or observed proportions are close to zero, as in the A-type sample ($n = 11$). Differences in disagreement rates among spectral classes were evaluated using a chi-square test of independence applied to the spectral-type versus agreement/disagreement contingency table. To distinguish the intrinsic behaviour of the two habitable-zone formulations from the spectral-type distribution of the observed exoplanet sample, habitable-zone boundary positions were also calculated as continuous functions of stellar effective temperature while fixing the stellar luminosity at

$$L = 1\,L_{\odot}\ .$$

The boundary divergence, defined as the difference between the habitable-zone boundary distances predicted by the Kopparapu and constant-flux models, provides a model-based measure of the influence of stellar effective temperature that is independent of the observed distribution of confirmed exoplanets.

3. Results

Among the 1,347 confirmed exoplanets included in this study, the conservative Kopparapu model classified 71 planets (5.27%) as residing within the habitable zone (HZ), whereas the simplified constant-flux model classified 46 planets (3.41%). The two models produced different classifications for 39 planets, corresponding to an overall disagreement rate of 2.90% (95% CI: 2.13–3.93%) (Table 1). Although the overall disagreement rate is modest, it demonstrates that HZ classification can depend on the choice of model for a measurable fraction of confirmed exoplanets.

Table 1. Overall HZ classification summary for the 1,347 confirmed exoplanets

Classification	N	% of sample
Total classified	1,347	100%
In HZ (Kopparapu, conservative)	71	5.27%
In HZ (constant-flux)	46	3.41%
Disagreement cases	39	2.90% (95% CI: 2.13–3.93%)

Fig. 1 presents the distribution of stellar luminosity and planetary orbital semi-major axis with the HZ boundaries from both models superimposed. As both approaches scale HZ distance with the square root of stellar luminosity, most planets are classified consistently because they lie well inside or well outside both HZ envelopes. In contrast, disagreement cases are concentrated within the narrow region separating the two boundary curves, where relatively small differences in boundary position are sufficient to change the HZ classification. These planets span a broad range of stellar luminosities but occur more frequently around lower-luminosity systems with shorter orbital distances.

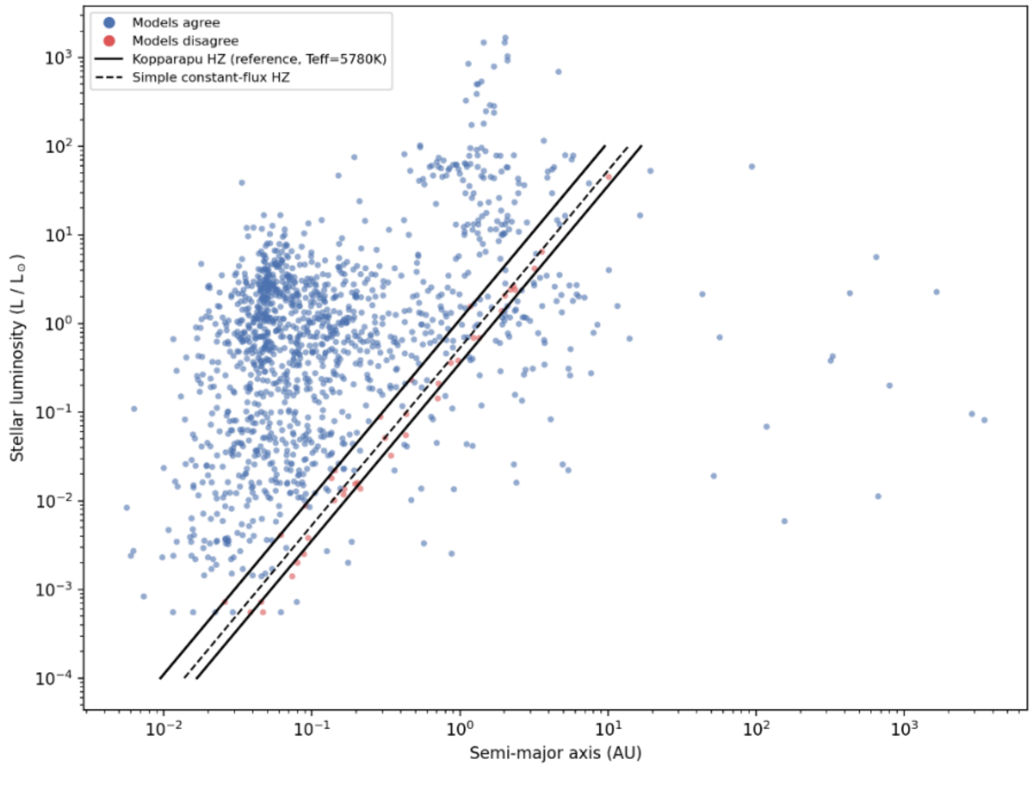

Fig. 1. Stellar luminosity versus planetary orbital semi-major axis for all 1,347 classified planets. Solid black curves denote the conservative Kopparapu HZ boundaries, while dashed curves denote the simplified constant-flux boundaries, both evaluated at $T_{\text{eff}} = 5780\text{K}$ for visualization. Blue points indicate agreement between the two models and red points indicate disagreement

The disagreement rate showed a clear dependence on host-star spectral type (Table 2). No disagreement was observed among the 11 A-type host stars, whereas the disagreement rate increased progressively from 0.48% for F-type stars to 1.54% for G-type stars, 2.68% for K-type stars, and 8.33% for M dwarfs. Fig. 2 illustrates this trend together with the corresponding 95% Wilson confidence intervals. The M-dwarf disagreement rate is substantially higher than the corresponding rates for the F- and G-type populations, while the broad confidence interval for A-type stars (0.00–25.88%) reflects the limited sample size rather than a distinct physical behaviour.

Table 2. HZ classification disagreement by host-star spectral type

Spectral type	n	Disagree	%	95% CI	Kopparapu more permissive	Constant-flux more permissive
A (≥7500 K)	11	0	0.00	0.00–25.88	0	0
F (6000–7500 K)	207	1	0.48	0.09–2.69	1	0
G (5200–6000 K)	454	7	1.54	0.75–3.15	7	0
K (3700–5200 K)	447	12	2.68	1.54–4.63	10	2
M (<3700 K)	228	19	8.33	5.40–12.65	14	5

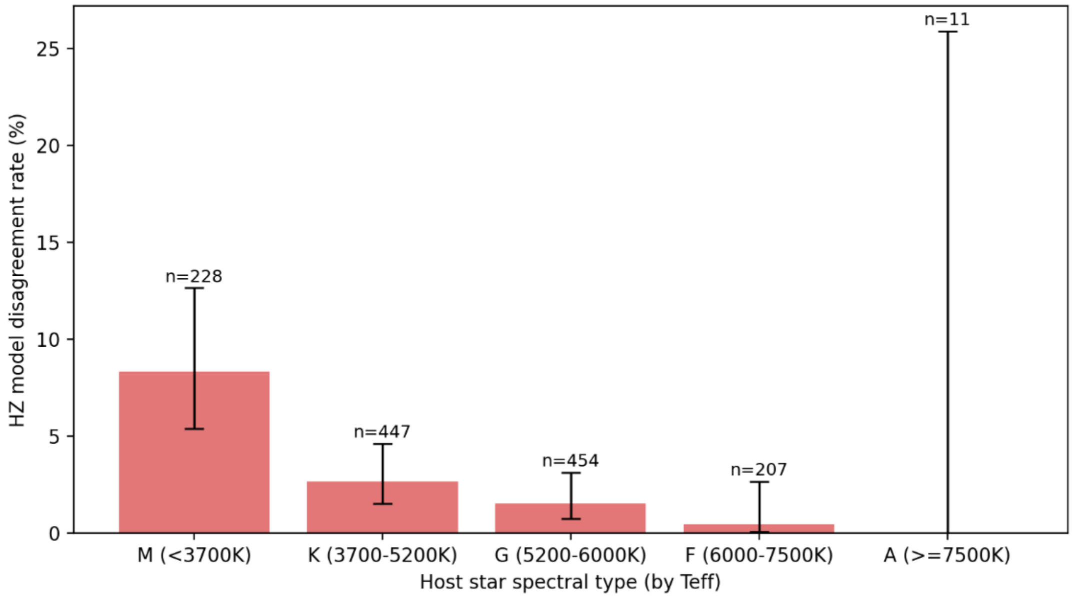

Fig. 2. HZ classification disagreement rate by host-star spectral type with 95% Wilson confidence intervals. Sample sizes are shown above each bar

The association between the disagreement rate and spectral type was statistically significant ($\chi^2 = 31.623$, dof = 4, $p < 0.0001$), indicating that disagreement between the two HZ formulations is not uniformly distributed across stellar types.

To examine this trend at finer temperature resolution, Fig. 3 compares the stellar effective-temperature distribution of the 39 disagreement cases with that of the complete sample. The overall exoplanet sample is centred around 5500–6000 K, whereas disagreement cases are shifted towards cooler stars, with prominent concentrations near 3300–3500 K and 4800–5000 K. Very few disagreement cases occur above approximately 6500 K, consistent with the spectral-type pattern observed in Table 2.

The direction of disagreement also varied with spectral type. Among the 19 disagreement cases around M-dwarf hosts, the Kopparapu model classified 14 planets (74%) as residing within the HZ, whereas the constant-flux model classified the same planets as outside the HZ; the reverse occurred for five planets. This indicates that disagreements around cool stars are predominantly associated with the temperature-dependent formulation identifying additional HZ candidates. To examine whether this pattern arises from the HZ models themselves rather than the distribution of observed exoplanets, HZ boundary divergence was calculated as a continuous function of stellar effective temperature while fixing stellar luminosity at $L = 1\,L_\odot$ (Fig. 4). The outer-boundary divergence is largest at low effective temperatures, decreases progressively towards approximately 8000 K, and increases again at higher temperatures. The inner boundary exhibits the same overall behaviour with smaller amplitude, crossing zero near the solar effective temperature (5780 K). The largest boundary divergence therefore occurs for cool stars, consistent with the higher disagreement rates observed for M-dwarf systems.

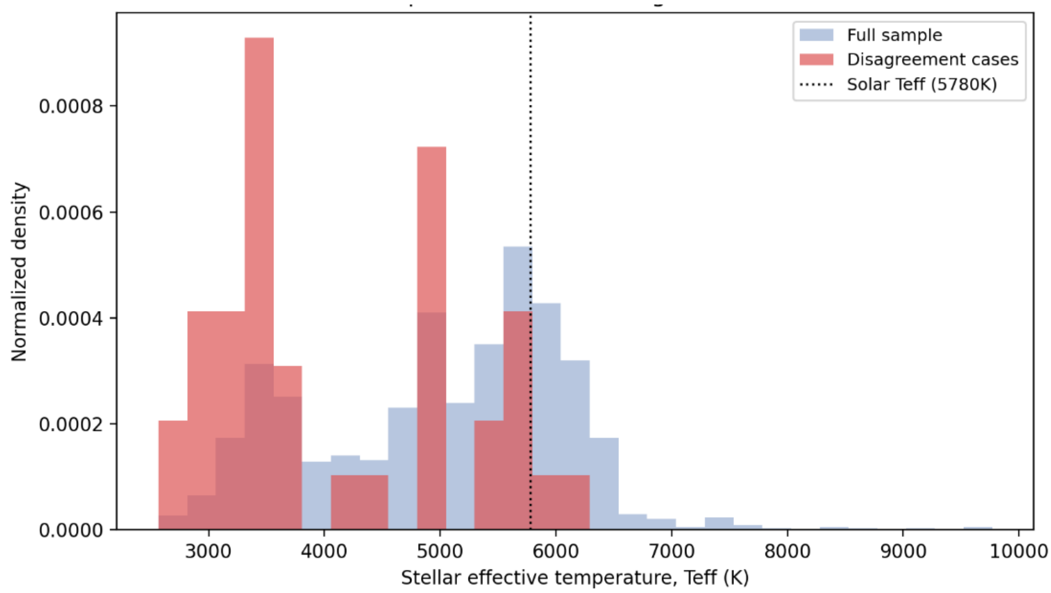

Fig. 3. Normalized distributions of host-star effective temperature for the complete sample (blue) and the 39 disagreement cases (red). The vertical dotted line marks the solar effective temperature (5780 K)

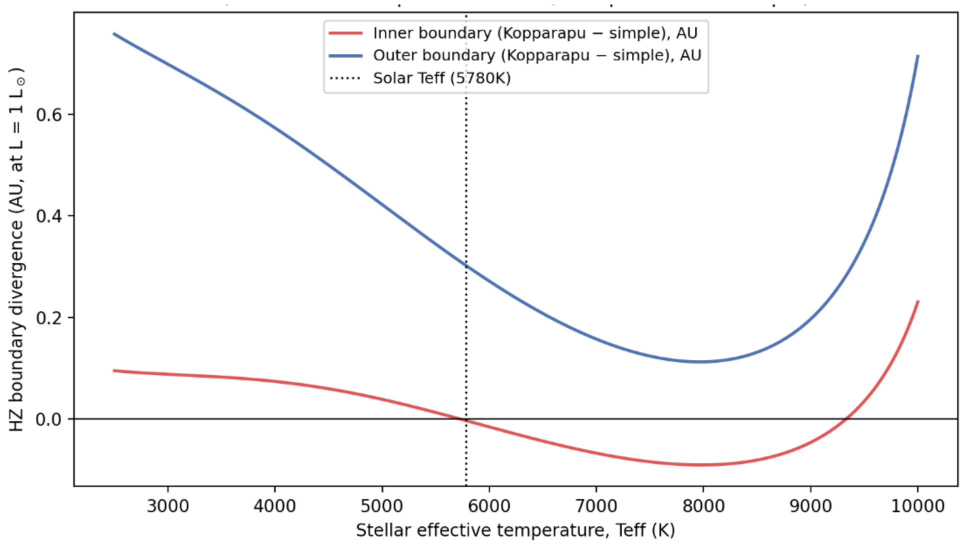

Fig. 4. Difference between the Kopparapu and constant-flux HZ boundary distances as a function of stellar effective temperature for $L = 1\,L_{\odot}$. The blue curve represents the outer boundary and the red curve the inner boundary

4. Discussion

The results show that the level of agreement between the temperature-dependent Kopparapu formulation and the simplified constant-flux model varies across stellar spectral types rather than remaining uniform. The disagreement rate increases from F- and G-type stars towards M dwarfs, consistent with the temperature dependence incorporated in the Kopparapu formulation (Kopparapu et al., 2013, 2014). As illustrated in Fig. 4, the difference between the two HZ formulations becomes larger as stellar effective temperature moves away from the solar reference temperature (5780 K), with the greatest divergence occurring for cool stars. This suggests that the observed spectral-type trend is primarily driven by the temperature-dependent correction included in the Kopparapu model. In the present comparison, the simplified constant-flux model adopts the same conservative solar reference effective stellar flux values reported by Kopparapu et al. (2013, 2014) but applies them uniformly to all host stars without the stellar effective-temperature correction. Consequently, the observed differences arise solely from the omission of the temperature-dependent component rather than from differences in the adopted reference habitable-zone limits. A physical explanation for this behaviour is provided by the different spectral energy distributions of stars. Cooler stars emit a larger fraction of their radiation at longer wavelengths, which affects how energy is absorbed and redistributed within planetary atmospheres. The Kopparapu formulation incorporates this effect through a temperature-dependent effective stellar flux, whereas the constant-flux model assumes the same solar reference flux limits for all stellar types. As a result, the two approaches become increasingly different for cool stellar hosts, leading to a higher frequency of disagreement for planets orbiting M dwarfs. This interpretation is also consistent with recent reviews of rocky exoplanet atmospheres and habitability, which emphasise the importance of stellar spectral energy distributions in determining planetary climate and habitable-zone boundaries (Wordsworth & Kreidberg, 2022). The direction of the disagreement is also noteworthy. Of the 19 disagreement cases around M-dwarf systems, the Kopparapu model classified 14 planets (74%) as residing within the habitable zone, while the constant-flux model classified them outside the HZ. This pattern suggests that simplified constant-flux criteria may exclude some planets that are identified as HZ candidates when the stellar temperature dependence is taken into account. Because M dwarfs are major targets in current searches for potentially habitable terrestrial planets owing to their observational accessibility and relatively high occurrence of small planets (Dressing & Charbonneau, 2015; Shields et al., 2016), differences between HZ formulations may influence the selection of targets for atmospheric characterisation and future observational surveys (Lagage et al., 2026; TRAPPIST-1 JWST Community Initiative, 2024). Systems such as TRAPPIST-1 further highlight the importance of accurately assessing habitable zones around cool stellar hosts (Gillon et al., 2017). These findings are consistent with the motivation behind the Kopparapu formulation. Earlier constant-flux models (Hart, 1979; Kasting et al., 1993) treated habitable-zone boundaries as independent of stellar effective temperature, whereas the Kopparapu model accounts for variations in stellar spectral energy distribution through a temperature-dependent effective stellar flux (Kopparapu et al., 2013, 2014). The present analysis complements these theoretical developments by examining how the choice of HZ formulation affects the classification of the current population of confirmed exoplanets. Previous studies have primarily focused on developing habitable-zone models (Kopparapu et al., 2013, 2014), compiling HZ planet catalogues (Bohl et al., 2026; Hill et al., 2023; Kane et al., 2016), or investigating planetary habitability around particular stellar populations (Hall et al., 2023; Jiang et al., 2024; Shields et al., 2016). In contrast, this study examines the level of agreement between two commonly used HZ formulations across the confirmed exoplanet catalogue. The observed disagreement rates therefore provide a quantitative measure of how model choice can influence HZ classification. Although the overall disagreement rate is relatively small (2.90%), it is concentrated among M-dwarf systems, which are a major focus of current and planned exoplanet surveys. Consequently, differences between HZ formulations may affect habitable-zone catalogues, estimates of potentially habitable planets, and the prioritisation of targets for detailed follow-up observations (Hill et al., 2023; Kane et al., 2016; Lagage et al., 2026). These results indicate that the choice of HZ formulation should be considered when comparing habitable-zone catalogues or interpreting classifications derived using different methodologies. One result should be interpreted with caution. No disagreement was observed among the 11 A-type host stars included in this study; however, the corresponding 95% Wilson confidence interval (0.00–25.88%) is broad because of the limited sample size. In addition, the model-level analysis indicates that HZ boundary divergence increases again at high stellar effective temperatures (Fig. 4), suggesting that disagreement may also occur for hotter stars. The absence of disagreement in the present dataset is therefore more likely related to the small number of confirmed planets around A-type stars than to complete agreement between the two formulations. Future observations and continued expansion of the confirmed exoplanet catalogue will help clarify this behaviour. Overall, the results indicate that the influence of HZ model selection is not the same across all stellar spectral types and is most evident for cool stars. Although the overall effect on the confirmed exoplanet population is modest, the concentration of disagreement among M-dwarf systems suggests that temperature-dependent HZ formulations can provide a more consistent basis for classifying planets around these stars and for supporting future habitable-zone catalogues and observational target selection (Hill et al., 2023; Lagage et al., 2026).

5. Conclusion

This study evaluated how the choice of habitable-zone (HZ) formulation influences the classification of confirmed exoplanets. Among 1,347 confirmed planets, the temperature-dependent Kopparapu model classified 71 planets (5.27%) as residing within the conservative HZ, whereas the simplified constant-flux model identified 46 planets (3.41%). The two approaches disagreed for 39 planets, corresponding to an overall disagreement rate of 2.90% (95% CI: 2.13–3.93%). The level of disagreement depended strongly on host-star spectral type, increasing from 0.48% for F-type stars and 1.54% for G-type stars to 2.68% for K-type stars and 8.33% for M dwarfs, with a statistically significant association ($\chi^2 = 31.623$, $p < 0.0001$). Among the 19 disagreement cases associated with M-dwarf systems, the temperature-dependent model classified 14 planets (74%) as residing within the habitable zone, whereas the constant-flux model classified these planets outside the HZ. These results indicate that differences between the two HZ formulations are concentrated among cool stellar hosts, where the temperature-dependent correction incorporated in the Kopparapu model has the greatest influence on habitable-zone boundaries. Although the overall disagreement across the confirmed exoplanet sample is relatively small, its concentration among M-dwarf systems suggests that HZ model selection can influence habitable-zone catalogues and the prioritisation of targets for future atmospheric characterisation. By providing a quantitative comparison of two commonly used habitable-zone formulations across the current confirmed exoplanet population, this study offers a useful reference for interpreting HZ classifications derived using different methodologies. The results also support the use of temperature-dependent HZ formulations when consistent classification across a wide range of stellar spectral types is required.

6. Limitations

This study has several limitations that should be considered when interpreting the results. First, HZ classifications were based on point estimates of stellar luminosity, stellar effective temperature, and planetary orbital semi-major axis obtained from the NASA Exoplanet Archive (Akeson et al., 2013). Measurement uncertainties associated with these parameters were not propagated into the analysis. Consequently, planets located close to habitable-zone boundaries may have uncertain classifications. Future studies could incorporate Monte Carlo uncertainty propagation to estimate classification probabilities and evaluate the robustness of HZ assignments for individual planets.

Second, the comparison was limited to the conservative habitable-zone boundaries defined by the Runaway Greenhouse and Maximum Greenhouse limits of Kopparapu et al. (2013, 2014). Alternative HZ definitions, including the optimistic Recent Venus and Early Mars limits, were not considered. Although the number of planets classified within the HZ may differ under these alternative definitions, evaluating their influence on model agreement was beyond the scope of the present study.

Third, the analysis represents a snapshot of the confirmed exoplanet population available in the NASA Exoplanet Archive as accessed on 18 July 2026. As new planets are discovered and stellar parameters are updated, the reported sample size and disagreement rates may change. Repeating this analysis with future catalogue releases will help assess the stability of the observed trends. Finally, this study compares only two widely used HZ formulations. Other habitable-zone models incorporating different atmospheric assumptions, cloud feedback, planetary mass, or climate processes have also been proposed (Selsis et al., 2007; Yang et al., 2013). Extending the present comparison to include additional HZ formulations would provide a broader assessment of model-dependent variation in habitable-zone classification.

Declaration of AI Use

The author hereby declares that no generative AI technologies, such as large language models (ChatGPT, COPILOT, etc.), and text-to-image generators have been used during the writing or editing of this manuscript.

Competing Interests

Author has declared that he/she has no known competing financial interests or non-financial interests or personal relationships that could have appeared to influence the work reported in this paper.

References

Akeson, R. L., Chen, X., Ciardi, D., Crane, M., Good, J., Harbut, M., Jackson, E., Kane, S. R., et al. (2013). The NASA Exoplanet Archive: Data and tools for exoplanet research. *Publications of the Astronomical Society of the Pacific, 125*(930), 989–999. https://doi.org/10.1086/672273

Bohl, A., Lawrence, L., Lowry, G., & Kaltenegger, L. (2026). Probing the limits of habitability: A catalogue of rocky exoplanets in the habitable zone. *Monthly Notices of the Royal Astronomical Society, 547*(3), stag028. https://doi.org/10.1093/mnras/stag028

Deb, S., Sharma, K., Biswas, S., & Medhi, B. J. (2025). Exploring the habitability and interior composition of exoplanets lying within the extended habitable zone. *Monthly Notices of the Royal Astronomical Society, 541*(2), 1180–1194. https://doi.org/10.1093/mnras/staf1057

Dressing, C. D., & Charbonneau, D. (2015). The occurrence of potentially habitable planets orbiting M dwarfs estimated from the full Kepler dataset and an empirical measurement of the detection sensitivity. *The Astrophysical Journal, 807*(1), 45. https://doi.org/10.1088/0004-637X/807/1/45

Gillon, M., Triaud, A. H. M. J., Demory, B.-O., Jehin, E., Agol, E., Deck, K. M., Lederer, S. M., de Wit, J., Burdanov, A., Ingalls, J. G., Bolmont, E., Leconte, J., Raymond, S. N., Selsis, F., Turbet, M., Barkaoui, K., Burgasser, A. J., Burleigh, M. R., Carey, S. J., … Queloz, D. (2017). Seven temperate terrestrial planets around the nearby ultracool dwarf star TRAPPIST-1. *Nature, 542*(7642), 456–460. https://doi.org/10.1038/nature21360

Hall, C., Stancil, P. C., Terry, J. P., & Ellison, C. K. (2023). A new definition of exoplanet habitability: Introducing the photosynthetic habitable zone. *The Astrophysical Journal Letters, 948*(2), L26. https://doi.org/10.3847/2041-8213/acccfb

Hart, M. H. (1979). Habitable zones about main sequence stars. *Icarus, 37*(1), 351–357. https://doi.org/10.1016/0019-1035(79)90141-6

Hill, M. L., Bott, K., Dalba, P. A., Fetherolf, T., Kane, S. R., Kopparapu, R., Li, Z., & Ostberg, C. (2023). A catalog of habitable zone exoplanets. *The Astronomical Journal, 165*(2), 34. https://doi.org/10.3847/1538-3881/aca1c0

Huang, S.-S. (1959). The problem of life in the universe and the mode of star formation. *Publications of the Astronomical Society of the Pacific, 71*(422), 421–424. https://doi.org/10.1086/127417

Jiang, J. H., Rosen, P. E., Liu, C. X., Wen, Q., & Chen, Y. (2024). Analysis of habitability and stellar habitable zones from observed exoplanets. *Galaxies, 12*(6), 86. https://doi.org/10.3390/galaxies12060086

Kane, S. R., Hill, M. L., Kasting, J. F., Kopparapu, R. K., Quintana, E. V., Barclay, T., Batalha, N. M., Borucki, W. J., Ciardi, D. R., Haghighipour, N., Hinkel, N. R., Kaltenegger, L., Selsis, F., & Torres, G. (2016). A catalog of Kepler habitable zone exoplanet candidates. *The Astrophysical Journal, 830*(1), 1. https://doi.org/10.3847/0004-637X/830/1/1

Kasting, J. F., Whitmire, D. P., & Reynolds, R. T. (1993). Habitable zones around main sequence stars. *Icarus, 101*(1), 108–128. https://doi.org/10.1006/icar.1993.1010

Kopparapu, R. K., Ramirez, R. M., SchottelKotte, J., Kasting, J. F., Domagal-Goldman, S., & Eymet, V. (2014). Habitable zones around main-sequence stars: Dependence on planetary mass. *The Astrophysical Journal Letters, 787*(2), L29. https://doi.org/10.1088/2041-8205/787/2/L29

Kopparapu, R. K., Ramirez, R., Kasting, J. F., Eymet, V., Robinson, T. D., Mahadevan, S., Terrien, R. C., Domagal-Goldman, S., Meadows, V., & Deshpande, R. (2013). Habitable zones around main-sequence stars: New estimates. *The Astrophysical Journal, 765*(2), 131. https://doi.org/10.1088/0004-637X/765/2/131

Lagage, P.-O., Mandell, A., Giménez, A., Angerhausen, D., Bolmont, E., Ducrot, E., Hu, R., & Roberge, A. (2026). The future of rocky worlds exploration. *Space Science Reviews, 222*, 40. https://doi.org/10.1007/s11214-026-01297-4

Liu, L.-G. (2018). Origin and early evolution of terrestrial planet atmospheres and oceans. *Physical Science International Journal, 20*(2), 1–8. https://doi.org/10.9734/PSIJ/2018/45815

Selsis, F., Kasting, J. F., Levrard, B., Paillet, J., Ribas, I., & Delfosse, X. (2007). Habitable planets around the star Gl 581? *Astronomy & Astrophysics, 476*(3), 1373–1387. https://doi.org/10.1051/0004-6361:20078091

Shields, A. L., Ballard, S., & Johnson, J. A. (2016). The habitability of planets orbiting M-dwarf stars. *Physics Reports, 663*, 1–38. https://doi.org/10.1016/j.physrep.2016.10.003

Spinelli, R., Borsa, F., Ghirlanda, G., Ghisellini, G., Haardt, F., & Rigamonti, F. (2024). The time evolution of the ultraviolet habitable zone. *Monthly Notices of the Royal Astronomical Society: Letters, 533*(1), L76–L82. https://doi.org/10.1093/mnrasl/slae064

TRAPPIST-1 JWST Community Initiative. (2024). A roadmap for the atmospheric characterization of terrestrial exoplanets with JWST. *Nature Astronomy, 8*(7), 810–818. https://doi.org/10.1038/s41550-024-02298-5

Van Looveren, G., Boro Saikia, S., Herbort, O., Schleich, S., Güdel, M., Johnstone, C., & Kislyakova, K. (2025). Habitable zone and atmosphere retention distance (HaZARD): Stellar-evolution-dependent loss models of secondary atmospheres. *Astronomy & Astrophysics, 694*, A310. https://doi.org/10.1051/0004-6361/202452998

Wordsworth, R., & Kreidberg, L. (2022). Atmospheres of rocky exoplanets. *Annual Review of Astronomy and Astrophysics, 60*(1), 159–201. https://doi.org/10.1146/annurev-astro-052920-125632

Yang, J., Cowan, N. B., & Abbot, D. S. (2013). Stabilizing cloud feedback dramatically expands the habitable zone of tidally locked planets. *The Astrophysical Journal Letters, 771*(2), L45. https://doi.org/10.1088/2041-8205/771/2/L45

Appendix A: Pseudocode

The following pseudocode summarizes the complete analysis pipeline described in Section 2, provided for reproducibility.

Appendix A: HZ Model Comparison Pipeline

Input: NASA Exoplanet Archive (ps table), accessed via TAP query

Output: Classification table, spectral-type summary, statistical tests

Step 1: Data Acquisition

```
QUERY archive.ps WHERE
   default_flag = 1
   AND st_teff IS NOT NULL
   AND st_lum IS NOT NULL
   AND pl_orbsmax IS NOT NULL
SELECT pl_name, hostname, st_teff, st_lum, pl_orbsmax

data <- results of QUERY
```

Step 2: Data Cleaning

```
FOR each row IN data:
   L_sun <- 10 ^ st_lum
   Teff  <- st_teff
   a_AU  <- pl_orbsmax

REMOVE rows WHERE:
   Teff <= 2500 OR Teff >= 10000
   OR a_AU <= 0
   OR L_sun <= 0

data <- cleaned rows
```

Step 3: Define Hz Model A (KOPPARAPU)

```
COEFFS <- {
   runaway_greenhouse: (S_sun=1.107, a=1.332e-4, b=1.580e-8,
                  c=-8.308e-12, d=-1.931e-15),
   maximum_greenhouse: (S_sun=0.356, a=6.171e-5, b=1.698e-9,
                  c=-3.198e-12, d=-5.575e-16)
}

FUNCTION kopparapu_Seff(Teff, boundary):
   (S_sun, a, b, c, d) <- COEFFS[boundary]
   T <- Teff - 5780
   RETURN S_sun + a*T + b*T^2 + c*T^3 + d*T^4

FUNCTION kopparapu_HZ(Teff, L):
   S_inner <- kopparapu_Seff(Teff, runaway_greenhouse)
   S_outer <- kopparapu_Seff(Teff, maximum_greenhouse)
   d_inner <- sqrt(L / S_inner)
   d_outer <- sqrt(L / S_outer)
   RETURN (d_inner, d_outer)
```

Step 4: Define Hz Model B (SIMPLE CONSTANT-FLUX)

```
FUNCTION simple_HZ(L, S_inner=1.1, S_outer=0.53):
    d_inner <- sqrt(L / S_inner)
    d_outer <- sqrt(L / S_outer)
    RETURN (d_inner, d_outer)
```

STEP 5: Classify Each Planet

```
FOR each planet IN data:
    (kop_in, kop_out)   <- kopparapu_HZ(planet.Teff, planet.L_sun)
    (simp_in, simp_out) <- simple_HZ(planet.L_sun)

    planet.in_HZ_kopparapu <- (kop_in <= planet.a_AU <= kop_out)
    planet.in_HZ_simple    <- (simp_in <= planet.a_AU <= simp_out)
    planet.agree           <- (planet.in_HZ_kopparapu == planet.in_HZ_simple)

n_total     <- COUNT(data)
n_kopparapu <- COUNT(planet.in_HZ_kopparapu == TRUE)
n_simple    <- COUNT(planet.in_HZ_simple == TRUE)
n_disagree  <- COUNT(planet.agree == FALSE)
```

Step 6: SPECTRAL-TYPE BINNING

```
FUNCTION spectral_type(Teff):
    IF Teff >= 7500: RETURN "A"
    ELIF Teff >= 6000: RETURN "F"
    ELIF Teff >= 5200: RETURN "G"
    ELIF Teff >= 3700: RETURN "K"
    ELSE: RETURN "M"
FOR each planet IN data:
    planet.spectral_type <- spectral_type(planet.Teff)
```

Step 7: Wilson Confidence Intervals

```
FUNCTION wilson_CI(successes, n, z=1.96):
    p <- successes / n
    denom <- 1 + z^2/n
    centre <- (p + z^2/(2*n)) / denom
    halfwidth <- (z/denom) * sqrt(p*(1-p)/n + z^2/(4*n^2))
    RETURN (centre - halfwidth, centre + halfwidth)
FOR each spectral_type_group IN GROUP(data BY spectral_type):
    n <- COUNT(group)
    n_dis <- COUNT(group.agree == FALSE)
    rate <- n_dis / n
    CI <- wilson_CI(n_dis, n)
    STORE (spectral_type, n, n_dis, rate, CI)
```

Step 8: Chi-Square Test of Independence

```
contingency_table <- CROSSTAB(spectral_type, agree)
(chi2, p_value, dof) <- CHI_SQUARE_TEST(contingency_table)
```

Step 9: Model-Level Boundary Divergence

```
L_fixed <- 1.0
```

```
FOR Teff_grid IN RANGE(2500, 10000, step=25):
   (kop_in, kop_out) <- kopparapu_HZ(Teff_grid, L_fixed)
   (simp_in, simp_out) <- simple_HZ(L_fixed)

   delta_inner <- kop_in - simp_in
   delta_outer <- kop_out - simp_out

   STORE (Teff_grid, delta_inner, delta_outer)
```

Step 10: Output

```
RETURN {
   classification_table,
   spectral_summary,
   chi2,
   p_value,
   dof,
   boundary_divergence_curve
}
```


Peer-review history:
The peer review history for this paper can be accessed here:
https://pr.sdiarticle5.com/review-history/163308